

Normalized Matching Transformer

Abtin Pourhadi Paul Swoboda
 Heinrich Heine University Düsseldorf
 {abtin.pourhadi, paul.swoboda}@hhu.de

Abstract

We present a new state of the art approach for sparse keypoint matching between pairs of images. Our method consists of a fully deep learning based approach combining a visual backbone coupled with a SplineCNN graph neural network for feature processing and a normalized transformer decoder for decoding keypoint correspondences together with the Sinkhorn algorithm. Our method is trained using a contrastive and a hyperspherical loss for better feature representations. We additionally use data augmentation during training.

This comparatively simple architecture combining extensive normalization and advanced losses outperforms current state of the art approaches on PascalVOC and SPair-71k datasets by 5.1% and 2.2% respectively compared to BBGM[31], ASAR [30], COMMON [20] and GMTR [33] while training for at least 1.7x fewer epochs.

Code and datasets are available at <https://github.com/Apollos1301/NormMatchTrans>.

1. Introduction

Traditional graph-matching pipelines [31, 37] rely on neural network backbones for computing discriminative features combined with combinatorial solvers to establish keypoint correspondences to address the feature matching problem. While effective, these approaches are often complex, requiring the combination of a neural network based feature computation stage with an intricate combinatorial stage for computing keypoint correspondences. Integrating the combinatorial stage into a neural network pipeline brings its own challenges, including non-differentiability and most often combinatorial solvers running on CPUs. Recent methods like GMTR [13], ASAR [30] and COMMON [20] proposed pure deep-learning approaches with a simpler Sinkhorn-based decoding. They have sought to enhance performance and robustness through transformer-based architectures, better losses and/or specialized regularization strategies. These newer approaches, while foregoing

a combinatorial stage, still outperform hybrid approaches, attesting to the strength of deep learning even in the setting of keypoint matching that has a strong combinatorial aspect to it.

While pure deep learning methods have already reached very high results on keypoint matching datasets, we show that there is still room for improvement. First, better backbones boost performance. We replace the commonly used VGG [33] backbone for a current swin-transformer [22]. Second, we process features at keypoints with a SplineCNN GNN [10], which adds helpful inductive biases incorporating the geometry of the keypoints to match. Third, we use transformers to mix information between and across images. We show that vanilla transformers can be outperformed by additional normalization techniques used in normalized transformers [23]. We argue that the employed normalization techniques are well-suited for our normalized feature representation: Instead of only normalizing at the end before doing cosine similarity and computing the losses, we normalize throughout, which helps in faster training and better overall performance. Our pipeline is trained using a contrastive [27] and hyperspherical [25] loss together with data augmentation.

Our work shows that the performance for keypoint matching, one of the classical and very well-studied problems in computer vision, has not yet saturated and can be enhanced by leveraging current deep learning methods. In particular, it seems that the combination of novel architectural improvements and training losses deliver improvements even in this relatively low data setting. Also no combinatorial subroutines are necessary given the capabilities of our neural network pipeline, simplifying our overall approach.

Contribution. In detail, our contributions are as follows:

Architecture: We propose a simple and efficient pure ML-based architecture combining an image processing backbone using a swin-transformer [22], followed by a keypoint feature processing stage consisting of SplineCNN [10], a graph neural network that exploits

the geometrical structure of keypoints.

Decoding: The feature computation stage is followed by a two-stream transformer decoder implemented using normalized transformers [23] for computing keypoint feature affinities followed by computing correspondences using the Sinkhorn algorithm [8]. Each decoder handles keypoints from one image. This design eliminates the need for combinatorial solvers leading to a simplified pipeline.

Loss: Our method incorporates improved loss formulations, including InfoNCE [27] and hyperspherical loss [25]. They improve feature embedding quality and ensure robust training, enabling the model to learn more discriminative representations.

Experimental: Extensive experiments demonstrate state-of-the-art performance on PascalVOC and SPair-71k datasets, with significant improvements over the state of the art methods BBGM [31], ASAR [30], COMMON [20] and GMTR [13] exceeding their performance by 5.1% on PascalVOC and 2.2% on SPair-71k. We also need at least $1.7x$ fewer epochs until training convergence than the baselines.

2. Related work

Related work on keypoint matching involves (i) *combinatorial* aspects for establishing a one-to-one correspondence between sets of keypoints, (ii) *hybrid* approaches that combine mainly neural networks for computing keypoint features with combinatorial routines to get correspondences and (iii) *pure deep learning* based methods that forego any combinatorial subroutines.

On the application side we distinguish between (i) *sparse* keypoint matching, which we study here, for computing correspondences between few select keypoints of distinct objects of the same class in different environments and (ii) *dense* keypoint matching for estimating homographies between many keypoints belonging to the same object in the same scene but e.g. viewed from different viewpoints.

Combinatorial Aspects & Assignment Problems. In the combinatorial literature the task of finding one-to-one correspondences between sets of points is called the assignment problem. When the cost function consists of only terms that measure how well two points match onto each other, we obtain the linear assignment problem. This problem is polynomially solvable and fast solvers for practical problems exist [1]. The Sinkhorn algorithm [8], an approximation to the linear assignment problem, is especially popular in machine learning, since it is easy to implement, can be differentiated through and runs on GPUs.

When additionally pairwise terms are used that measure how well pairs of points match to each other we obtain the quadratic assignment problem, also known as graph matching in the computer vision literature. In the keypoint matching scenario the quadratic assignment problem allows to incorporate geometric information, e.g. penalizing matching keypoints that are nearby in one image to ones that are far away from each other in the other image etc. From a computational standpoint, the quadratic assignment problem is much more involved. Current state of the art solvers [14, 15, 17, 35, 37, 46] are complex and, while relatively fast, still present a computational bottleneck. From a theoretical viewpoint the quadratic assignment problem is a well known NP-hard problem [19] and notoriously difficult in practice [4].

Extensions for computing correspondences between multiple (≥ 3) sets of keypoints that take into account the ensuing cycle consistency are known under the name permutation synchronization [2, 28] or multi-graph matching [7, 17, 36].

Hybrid Approaches. For the keypoint matching problem the traditional approach is to first extract discriminative features for each keypoint (resp. for pairs of keypoints), use those to compute costs for matching keypoints and finally to compute correspondences using the linear or quadratic assignment problem. Some approaches use ad-hoc heuristics for decoding correspondences, e.g. via reformulation to constrained vertex classification [41] or the quadratic assignment problem [31, 37, 41].

Pre-neural network approaches with hand-crafted feature descriptors were for quite some time still state of the art [37]. However, neural network features eventually overtook [44]. Follow-up work NGM [41] differentiates through the construction of a quadratic assignment problem and decodes the matching by converting to a constrained vertex classification problem. The hybrid approach [31] combined a state of the art neural network pipeline with a quadratic assignment solver and used a special backpropagation technique [39] to learn in tandem with the non-differentiable combinatorial solver.

Pure Deep-Learning. When not using combinatorial routines it is even more important to obtain discriminative features. One of the first pure neural network methods [44] relaxed a graph matching solver to be differentiable and used feature hierarchies. PCA [40] differentiates end-to-end and learns linear and quadratic affinity costs. QCDGM [12] proposes a differentiable quadratic constrained-optimization compatible with a deep learning optimizer and a balancing term in the loss function GLMNet [16] utilizes a GNN and alleviates oversmoothing by utilizing an anisotropic Laplacian "sharpening" operation. CIE [42] employs attention

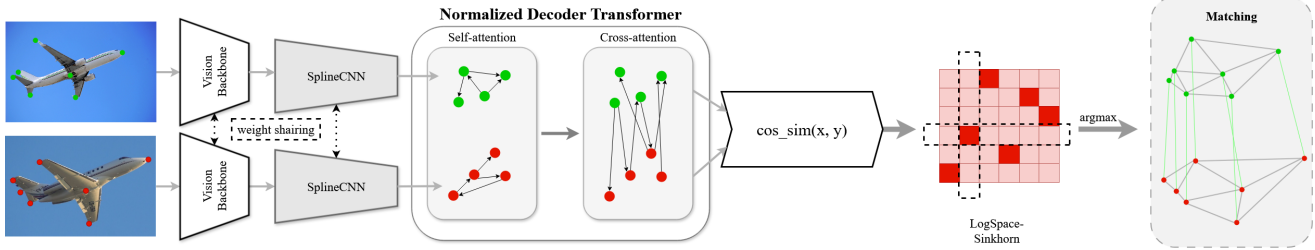


Figure 1. Normalized matching transformer inference. A pair of images is passed each through a swin-transformer visual backbone. Features at keypoints are extracted and given through a SplineCNN for further feature refinement. A normalized transformer decoder interleaves self-attention between keypoint features from the same image with cross-attention that mixes information across images. Finally, cosine similarities are computed and given as affinities to a logspace Sinkhorn routine from which a matching is decoded.

and improves upon plain attention by enforcing channel independence and sparsity in the ensuing matching decoding step. DGMC [11] uses the graph neural network [10] and an ad-hoc message passing routine for obtaining correspondences. COMMON [20] likewise uses SplineCNN and trains using contrastive losses. ASAR [30] improves performance by using adversarial training and an advanced regularization technique. GMTR [13] uses a transformer architecture with self- and cross-attention to exchange information between keypoints in the same and different images.

Our approach differs from previous work in jointly combining a strong backbone, transformer based architecture with contrastive and hyperspherical representation learning and hyperspherical normalization throughout the transformer. These were not or not jointly used before. We show that this combination achieves better performance while needing a shorter training.

In the closely related area of dense keypoint matching, transformer based architectures [21, 32, 34] have become state of the art as well.

3. Method

Our method consists of five building blocks:

Visual feature extraction: Visual features are extracted from the images using a pre-trained swin-transformer [22] backbone.

GNN: Keypoints are treated as nodes to construct an undirected graph from the visual features. A SplineCNN [10] is employed to refine the node features by aggregating local spatial information. This approach was pioneered in [11].

Normalized transformer: The normalized Transformer (nGPT) [23] architecture is used with self-attention layers for exchanging information between keypoints of the same image and cross-attention layers for exchanging information between keypoints from different layers.

Sinkhorn matching: Using the refined features we compute cosine similarities between pairs of keypoints from each image. This similarity score matrix is passed through a logspace-sinkhorn algorithm for ensuring a double stochastic matrix. Each index of the maximum in each row indicates the best possible match between the source (row) and target (column) node.

InfoNCE and hyperspherical losses: We use InfoNCE [27] and hyperspherical [24] loss functions for shaping better feature representations. InfoNCE aligns features for the corresponding keypoints in different images and penalizes alignment of non-corresponding features. The hyperspherical loss distributes keypoint features from the same image uniformly on the hypersphere, ensuring more distinctive features. For better results we apply the hyperspherical loss after each normalized transformer layer.

An illustration of our approach is provided in Figure 1 for the inference and 2 and 3 for losses during training.

Visual Feature Extraction. We are given two images I^1, I^2 alongside coordinates k_1^1, \dots, k_m^1 and k_1^2, \dots, k_m^2 specifying the m keypoint positions in each image. We pass both images through a swin-transformer [22] and obtain down-sampled features. The spatial features corresponding to the specified keypoints are interpolated from these down-sampled features using a bilinear sampling technique. For each keypoint we extract features from the last and second last layer of the backbone and concatenate them. Following BBGM [31] we additionally mean-pool all features from the backbone to get a global feature for each image that helps to class-condition the matching process.

We use the swin-large version as backbone.

GNN. To incorporate the spatial structure of the objects as indicated by the geometry of the keypoints, we use a SplineCNN [10] as suggested in [11]. We construct a graph

with nodes being keypoints and edges coming from a Delaunay triangulation. Two rounds of graph convolution are performed to refine feature representations for each image separately. Unlike general-purpose GNNs that focus on aggregating features across nodes without explicit consideration of their spatial layout, SplineCNN utilizes spline-based kernels that adapt to the graph’s Euclidean geometry, allowing for a better representation of spatial interactions.

The GNN operates on a message-passing paradigm, where node features are iteratively updated by aggregating information from neighboring nodes at each layer. Trainable B-Spline kernels anisotropically convolve features from other nodes.

Our implementation employs two spline convolution layers, each with a kernel size of 5 and utilizes max aggregation. We use ReLU as non-linearity. We use Euclidean coordinates for the geometric input to the trainable B-splines.

Normalized Transformer. The normalized transformer [23], a variant of the original transformer architecture [38], uses hyperspherical normalization and projects intermediate and final representations back to unit norm. This aligns well with the graph matching setting where we want to measure potential correspondences by cosine similarity of their (implicitly normalized) features. Experiments in NLP have demonstrated that the normalized transformer architecture can converge faster, be numerically more stable and can reach better solutions.

In particular, the normalized transformer uses normalization after attention, the MLP block and the residual connections. Let $f = f_1, \dots, f_m$ be a feature sequence coming from all the keypoints in an image. For cross-attention let f_{other} be the keypoint feature sequence from the other image. Then normalized self-attention, cross-attention and MLP layers can be written as

Norm. Self-Attn(f):
$f_A \leftarrow \text{Norm}(\text{Self-Attn}(f))$
$f \leftarrow \text{Norm}(f + \alpha_A \cdot (f_A - f))$
Norm. Cross-Attn(f, f_{other}):
$f_A \leftarrow \text{Norm}(\text{Cross-Attn}(f, f_{other}))$
$f \leftarrow \text{Norm}(f + \alpha_C \cdot (f_A - f))$
Norm. MLP(f):
$f_M \leftarrow \text{Norm}(\text{MLP}(f))$
$f \leftarrow \text{Norm}(f + \alpha_M \cdot (f_M - f))$

Normalized transformer primitives.

Element-wise step sizes $\alpha_A, \alpha_C, \alpha_M$ in residual connections are learned positive vectors.

A transformer layer in our matching method consists of first doing normalized self-attention separately for keypoint features of each image, then doing two normalized cross-attention passes where one keypoint feature sequence attends to the other respectively and finally passing through a normalized MLP block. Additionally, after cross-attention we element-wise modulate keypoint features with the global feature token and normalize afterwards to unit norm again.

We use 4 such two-stream normalized transformer decoder layers using 12 heads with a feature dimension of 648. We use SiLU activations.

Sinkhorn Matching. To establish correspondences between keypoints, we first compute cosine similarities between each pair of features coming from different images. This square affinity matrix is given to the Sinkhorn algorithm, which outputs a double stochastic matrix. To decode final correspondences, we use the computed double stochastic matrix and go through each row i and pick the column j with maximum entry, meaning that keypoint i in the first image is matched to keypoint j in the second one.

Our full matching pipeline is detailed in Algorithm [Normalized Matching Transformer](#).

Normalized Matching Transformer	
Input: Input images I^1, I^2 , keypoints $k_1^1, \dots, k_m^1, k_1^2, \dots, k_m^2$	
Output: Matching $\pi : [m] \rightarrow [m]$	
// Swin-transformer backbone	
$g_1^i, \dots, g_n^i = \text{Backbone}(I^i)$	$\forall i \in [2]$
// Global feature token	
$f_{global}^i = \text{Avg-Pool}(f_1^i, \dots, f_n^i)$	$\forall i \in [2]$
// Interpolate features at keypoint	
$f_j^i = \text{Interp}(g^i, k_j)$,	$\forall i \in [2], j \in [m]$
// SplineCNN GNN	
$f^i = f_1^i, \dots, f_m^i = \text{GNN}(f_1^i, \dots, f_m^i)$	$\forall i \in [2]$
// Normalized Transformer Decoder	
for $iter = 1, \dots, L$ do	
$f^i = \text{Norm. Self-Attn}(f^i, f_{global}^i)$	
$f^1 = \text{Norm. Cross-Attn}(f^1, f^2)$	
$f^2 = \text{Norm. Cross-Attn}(f^2, f^1)$	
$f_j^i = \text{Norm}(f_j^i \cdot f_{global}^i)$	$i \in [2], j \in [m]$
$f^i, f_{global}^i = \text{Norm. MLP}(f^i, f_{global}^i)$	$\forall i \in [2]$
// Sinkhorn matching	
$C_{ij} = \text{cos sim}(f_i^1, f_j^2)$	$\forall i, j \in [m]$
$A = \text{Sinkhorn}(C)$	
$\pi(i) = \arg \max_{j \in [m]} \{A_{ij}\}$	$\forall i \in [m]$

Training Losses. We use the contrastive InfoNCE loss introduced in [27] for better feature representations. Cor-

responding points are treated as positive pairs, while non-corresponding matches from the other image are treated as negative ones. This leads to matching keypoints having aligned representations with large cosine similarity while non-matching ones having low cosine similarity.

In particular, let f_i^1 and f_j^2 be two matching keypoints features coming out of the transformer decoder. Let f_i^1 and $f_l^2, l \in [m] \setminus \{j\}$ be the keypoint features in image 2 that do not match to f_i^1 . Then the InfoNCE loss is

$$\mathcal{L}_{\text{InfoNCE}} = -\log \frac{\exp(\cos \text{sim}(f_i^1, f_j^2)/\tau)}{\sum_{l \in [m] \setminus \{j\}} \exp(\cos \text{sim}(f_i^1, f_l^2)/\tau)}, \quad (1)$$

Here $\tau > 0$ is a learnable parameter. The overall InfoNCE loss is then the summation of the InfoNCE losses over all keypoints features. To symmetrize, we also take the matches the other way around.

To further encourage separation between keypoint features coming from the same image and to promote a more uniform distribution of features on the hypersphere we use a hyperspherical loss [25]. Let

$$C = (\cos \text{sim}(f_i^1, f_j^2))_{i,j \in [m]} \in \mathbb{R}^{m \times m}. \quad (2)$$

be the matrix of all pairwise cosine similarities. Then the hyperspherical loss is

$$\mathcal{L}_{\text{HS}} = \frac{1}{m} \sum_{i=1}^m \max_j \{C_{ij} - 2 \cdot \mathbf{1}_{\{i=j\}}\}. \quad (3)$$

This loss penalizes whenever two different keypoints are aligned. The diagonal subtraction $-2 \cdot \mathbf{1}_{\{i=j\}}$ ensures that this penalization is not carried out for the same keypoint.

We also incorporate the hyperspherical loss as an auxiliary layer loss on every matching transformer layer. In our approach, the loss is weighted using a parameter $p = 0.3$ that increases linearly with the layer depth. Then the loss is

$$\mathcal{L}_{\text{HS}}^{\text{layer}} = \sum_{k=1}^L k \cdot p \cdot \mathcal{L}_{\text{HS}}^{(k)}, \quad (4)$$

where p is the weighted hyperparameter and $\mathcal{L}_{\text{HS}}^{(k)}$ is the layer wise hyperspherical loss. This progressive weighting ensures that deeper layers, which contribute more critically to the final feature representations, receive a stronger regularization. We then average over the two decoders to obtain a single layer-wise loss and add that to the overall hyperspherical loss computed from the final decoder outputs. Consequently, this strategy encourages a more uniform distribution of keypoint features on the hypersphere across all layers, ultimately leading to enhanced feature distinctiveness and improved matching performance.

Our overall loss sums up the InfoNCE and hyperspherical loss without any weighting.

An illustration of the loss construction is given in Figures 2 and 3.

4. Experiments

Parameter	Value
Swin-Large	
image size	384
patch size	4
window size	24
embedding dimension	128
SplineCNN	
input features	1024
output features	648
# layers	2
kernel size	5
Transformer	
model dim, d_{model}	648
# heads	12
# decoder layers	4
MLP hidden mult	4
Activation	SiLU
layer loss param	0.3
Training	
Batch size (PascalVOC)	8
Batch size (SPair-71k)	5
# Epochs	6
Learning rate	5×10^{-4}

Table 1. Default hyperparameters for swin transformer, SplineCNN, normalized transformer, and training settings.

Training Details. Our network is trained using the Adam optimizer [18]. The initial learning rate for the network is set to 5×10^{-4} , while the swin-transformer [22] backbone with layer normalization uses a learning rate scaled down by a factor of 0.03. Additional normalization was omitted due to the inherent design of the normalized transformer. The learning rate is scaled by a factor of 0.1 after epoch 2 and 5. For PascalVOC the batch size of image pairs is set to 8 and for Spair-71k the batch size is set to 5. Our validation set is obtained by taking 1000 image pairs per class. We use augmentations provided through the Albumentations package [5]. Specifically, we use Mixup [45], Cutmix [43] and Random Erasing [47]. The model is run on two GPUs by using torch’s Distributed library. Other hyperparameters are listed in Table 1.

It is noteworthy that we only need 6 epochs to train, while BBGM [31] needs 10, ASAR [30] 16 and COM-MON [20] 16. Even though time per epoch might not be comparable, since the normalized transformer needs some-

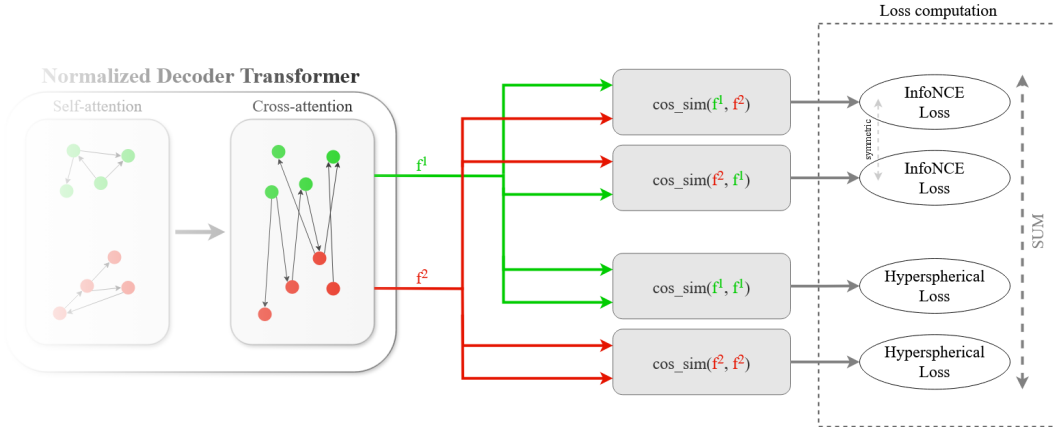


Figure 2. Normalized matching transformer losses. Losses are applied on the features that are computed by the normalized transformer decoder. InfoNCE losses are computed on cosine similarities of features coming from a single keypoint in one image and all keypoint features from the other one and align matching correspondences. For symmetry we apply the InfoNCE loss in both directions. For distributing features of different keypoints in the same image we use a hyperspherical loss on the keypoint features coming from each image separately.

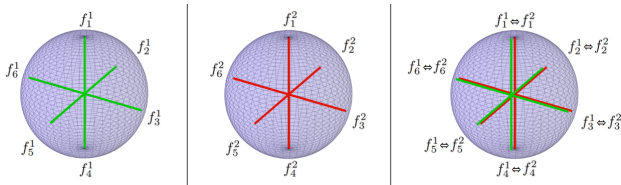


Figure 3. Geometric illustration of hyperspherical and InfoNCE losses. The hyperspherical losses (two left spheres) from (4) distributes different keypoint features f_j^i for different keypoints $j \in [m]$ and each image $i \in [2]$ across the hypersphere and is applied to each image separately. The InfoNCE (right side) loss from (1) aligns features $f_j^1 \leftrightarrow f_j^2$ from matching keypoints (assuming the matching is identity here) from different images.

what more time due to worse kernel fusion as compared to a vanilla transformer, this reveals significant possible training time savings on a more optimized normalized transformer implementation.

Datasets. We train and test on PascalVOC and SPair-71k, the two most challenging current sparse keypoint matching datasets. We opted to forego e.g. Willow Object Class [6] and other similar datasets since performance of previous works is already almost perfect there.

PascalVOC: We use PascalVOC [9] images with Berkeley annotations [3]. Images are from 20 classes and are of size 256×256 . Up to 23 keypoints are contained in each image. In order to be comparable to other works we use standard intersection filtering, i.e. when matching we only include keypoints that are in both images

and discard outliers.

SPair-71k: The SPair-71k dataset [26] is a successor to PascalVOC and offers higher image quality and keypoint annotation and removal of problematic and poorly annotated image categories. It contains 70.958 image pairs. Images are taken from PascalVOC and Pascal3D+.

Baselines. We compare our results with the highest-performing baselines from the literature, to the best of our knowledge.

PCA [40]: End-to-end differentiable deep network pipeline to learn linear and quadratic affinity costs for graph matching with graph embedding models.

GLMNet [16]: GNN-method using Laplacian sharpening.

CIE [42]: Channel independent and sparsity inducing graph embedding method.

DGMC [11]: Deep Graph Matching Consensus using SplineCNN and an iterative message passing consensus routine.

BBGM [31]: Hybrid VGG/SplineCNN backbone and quadratic assignment solver for establishing correspondences trained end-to-end with the optimization solver in the loop.

NGM [41]: Learn quadratic assignment problem costs via an embedding network and solve it via constrained vertex classification.

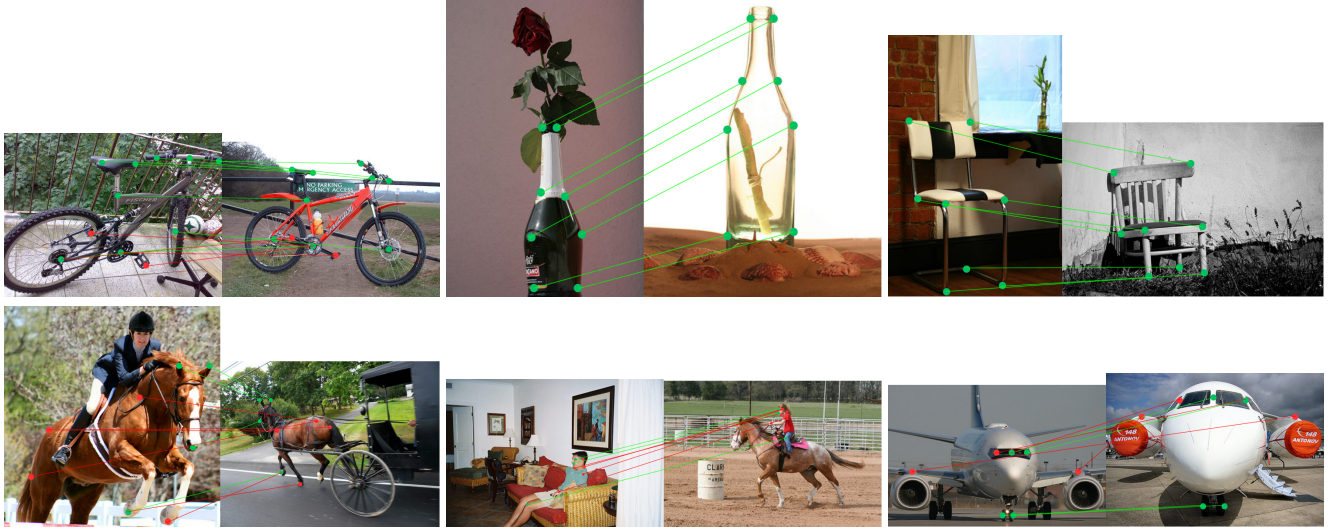


Figure 4. Qualitative results of selected keypoint matchings from the SPair-71k [26] dataset. The top row depicts perfect matchings, while the bottom row shows a few failure cases.

Method	✈️	🚲	🦋	🚗	🔪	🚚	🚙	🐎	🏠	🐘	🐪	🐴	🐎	🚲	🚶	🌱	🐕	🚗	🚚	🚚	Mean
GMN-PL [29]	31.1	46.2	58.2	45.9	70.6	76.5	61.2	61.7	35.5	53.7	58.9	57.5	56.9	49.3	34.1	77.5	57.1	53.6	83.2	88.6	57.9
PCA [40]	40.9	55.0	65.8	47.9	76.9	77.9	63.5	67.4	33.7	66.5	63.6	61.3	58.9	62.8	44.9	77.5	67.4	57.5	86.7	90.9	63.8
NGM [41]	50.8	64.5	59.5	57.6	79.4	76.9	74.4	69.9	41.5	62.3	68.5	62.2	62.4	64.7	47.8	78.7	66.0	63.3	81.4	89.6	66.1
GLMNet [16]	52.0	67.3	63.2	57.4	80.3	74.6	70.0	72.6	38.9	66.3	77.3	65.7	67.9	64.2	44.8	86.3	69.0	61.9	79.3	91.3	67.5
CIE [42]	51.2	69.2	70.1	55.0	82.8	72.8	69.0	74.2	39.6	68.8	71.8	70.0	71.8	66.8	44.8	85.2	69.9	65.4	85.2	92.4	68.9
DGMC [11]	50.4	67.6	70.7	70.5	87.2	85.2	82.5	74.3	46.2	69.4	69.9	73.9	73.8	65.4	51.6	98.0	73.2	69.6	94.3	89.6	73.2±0.5
BBGM [31]	61.5	75.0	78.1	<u>80.0</u>	87.4	93.0	89.1	80.2	58.1	77.6	76.5	79.3	78.6	78.8	66.7	97.4	76.4	77.5	97.7	<u>94.4</u>	80.1±0.6
GMTR [13]	<u>69.0</u>	74.2	<u>84.1</u>	75.9	87.7	<u>94.2</u>	<u>90.9</u>	<u>87.8</u>	<u>62.7</u>	<u>83.5</u>	<u>93.9</u>	<u>84.0</u>	78.7	<u>79.6</u>	<u>69.2</u>	99.3	<u>82.5</u>	<u>83.0</u>	<u>99.1</u>	93.3	83.6
COMMON [20]	65.6	<u>75.2</u>	80.8	79.5	<u>89.3</u>	92.3	90.1	81.8	61.6	80.7	95.0	82.0	<u>81.6</u>	79.5	66.6	<u>98.9</u>	<u>78.9</u>	80.9	99.3	93.8	82.7
NMT (ours)	75.8	81.9	90.9	82.4	93.5	95.4	92.7	90.7	84.6	85.2	92.9	89.3	89.4	86.9	77.2	98.5	85.8	88.0	97.6	95.5	88.7

Table 2. Average accuracy (%) of each object category on Pascal VOC. Best results are **bold** and second best are underlined.

Method	✈️	🚲	🦋	🚗	🔪	🚚	🚙	🐎	🏠	🐘	🐪	🐴	🐎	🚲	🚶	🌱	🐕	🚗	🚚	🚚	Mean
DGMC [11]	54.8	44.8	80.3	70.9	65.5	90.1	78.5	66.7	66.4	73.2	66.2	66.5	65.7	59.1	98.7	68.5	84.9	98.0	72.2	72.2	
BBGM [31]	66.9	57.7	85.8	78.5	66.9	95.4	86.1	74.6	68.3	78.9	73.0	67.5	79.3	73.0	99.1	74.8	95.0	98.6	78.9	78.9	
GMTR [13]	75.6	67.2	<u>92.4</u>	76.9	69.4	94.8	89.4	77.5	72.1	<u>86.3</u>	77.5	72.2	86.4	<u>79.5</u>	<u>99.6</u>	84.4	96.6	99.7	83.2	83.2	
COMMON [20]	<u>77.3</u>	<u>68.2</u>	92.0	<u>79.5</u>	<u>70.4</u>	<u>97.5</u>	<u>91.6</u>	82.5	<u>72.2</u>	88.0	<u>80.0</u>	<u>74.1</u>	<u>83.4</u>	82.8	99.9	84.4	<u>98.2</u>	<u>99.8</u>	<u>84.5</u>	<u>84.5</u>	
NMT (ours)	79.3	72.7	94.9	84.2	74.8	98.7	94.4	<u>82.2</u>	81.1	88.0	85.5	81.3	82.3	79.4	<u>100</u>	<u>83.2</u>	99.2	99.9	86.7	86.7	

Table 3. Average accuracy (%) of each object category on SPair-71k. Best results are **bold** and second best are underlined.

ASAR [30]: Adversarial training based on model [41].

COMMON [20]: VGG/SplineCNN based method trained with contrastive losses and momentum distillation.

GMTR [13]: Graph Matching Transformer using self- and cross-attention.

NMT (Ours): Our normalized matching transformer approach as detailed in Algorithm .

Results. Class-specific and overall results in terms of matching accuracy are presented in Table 2 for PascalVOC and in Table 3 for SPair-71k. Selected qualitative examples are shown in Figure 4.

On PascalVOC we outperform on average the baselines by 5.1%. We are better on 17 out of 20 image categories.

On SPair-71k we overall outperform all baselines by 2.2% matching accuracy. We are better on 13 out of 18 image categories and second best on 3.

Ablations. We provide ablations on our main architectural and training contributions on PascalVOC. The results are summarised in Table 4. We see that all contributions significantly add to final performance. The main performance driver are our losses, followed by improved backbone, normalized transformer and augmentations. Augmentations, while giving 1.2%, are still significant, but not overly so.

We have experimented with other simple pixel-wise augmentations like changing saturation value, random gamma, RGB shift etc., which however degraded performance.

Method	PascalVOC
NMT (FULL)	88.7%
w/o augmentation	-1.2%
w/o layer loss	-0.8%
w/ vanilla transformer	-2.6%
w/ cross entropy Loss	-15.1%
w/ VGG16	-4.9%

Table 4. Ablation study on PascalVOC. We ablate augmentations, replacing the normalized transformer by a vanilla one, replacing InfoNCE and hyperspherical loss by cross entropy and replacing the swin-transformer backbone with VGG [33].

5. Conclusion

We have shown that the combination of advances in transformer design coupled with representation learning losses leads to significant gains in two very competitive keypoint matching benchmarks. We argue that normalization throughout our neural networks is helpful in the context of keypoint matching, where typically only the output features have been normalized. This has led to fast training and superior performance. We conjecture that pursuing normalization together with representation learning in other related computer vision applications might also lead to improvements.

6. Acknowledgments

We thank Anirudh Yadav for sharing parts of the codebase with us. Also special thanks to Kira Maag for pre-reviewing this work.

References

- [1] Ravindra K Ahuja, Thomas L Magnanti, James B Orlin, et al. *Network flows: theory, algorithms, and applications*. Prentice hall Englewood Cliffs, NJ, 1993. 2
- [2] Florian Bernard, Daniel Cremers, and Johan Thunberg. Sparse quadratic optimisation over the stiefel manifold with application to permutation synchronisation. *Advances in Neural Information Processing Systems*, 34:25256–25266, 2021. 2
- [3] Lubomir Bourdev and Jitendra Malik. Poselets: Body part detectors trained using 3d human pose annotations. In *2009 IEEE 12th international conference on computer vision*, pages 1365–1372. IEEE, 2009. 6
- [4] Rainer E Burkard, Stefan E Karisch, and Franz Rendl. Qaplib—a quadratic assignment problem library. *Journal of Global optimization*, 10:391–403, 1997. 2
- [5] Alexander Buslaev, Vladimir I. Iglovikov, Eugene Khvedchenya, Alex Parinov, Mikhail Druzhinin, and Alexandr A. Kalinin. Albumentations: Fast and flexible image augmentations. *Information*, 11(2), 2020. 5
- [6] Minsu Cho, Karteek Alahari, and Jean Ponce. Learning graphs to match. In *Proceedings of the IEEE International Conference on Computer Vision*, pages 25–32, 2013. 6
- [7] Yves Crama and Frits CR Spijksma. Approximation algorithms for three-dimensional assignment problems with triangle inequalities. *European Journal of Operational Research*, 60(3):273–279, 1992. 2
- [8] Marco Cuturi. Sinkhorn distances: Lightspeed computation of optimal transport. *Advances in neural information processing systems*, 26, 2013. 2
- [9] Mark Everingham, Luc Van Gool, Christopher KI Williams, John Winn, and Andrew Zisserman. The pascal visual object classes (voc) challenge. *International journal of computer vision*, 88:303–338, 2010. 6
- [10] Matthias Fey, Jan Eric Lenssen, Frank Weichert, and Heinrich Müller. Splinecnn: Fast geometric deep learning with continuous b-spline kernels. In *Proceedings of the IEEE conference on computer vision and pattern recognition*, pages 869–877, 2018. 1, 3
- [11] Matthias Fey, Jan E Lenssen, Christopher Morris, Jonathan Masci, and Nils M Kriege. Deep graph matching consensus. *arXiv preprint arXiv:2001.09621*, 2020. 3, 6, 7
- [12] Quankai Gao, Fudong Wang, Nan Xue, Jin-Gang Yu, and Gui-Song Xia. Deep graph matching under quadratic constraint. In *Proceedings of the IEEE/CVF conference on computer vision and pattern recognition*, pages 5069–5078, 2021. 2
- [13] Jinpei Guo, Shaofeng Zhang, Runzhong Wang, Chang Liu, and Junchi Yan. Gmtr: Graph matching transformers. In *ICASSP 2024-2024 IEEE International Conference on Acoustics, Speech and Signal Processing (ICASSP)*, pages 6535–6539. IEEE, 2024. 1, 2, 3, 7
- [14] Stefan Haller, Lorenz Feineis, Lisa Hutschenreiter, Florian Bernard, Carsten Rother, Dagmar Kainmüller, Paul Swo-boda, and Bogdan Savchynskyy. A comparative study of graph matching algorithms in computer vision. In *European Conference on Computer Vision*, pages 636–653. Springer, 2022. 2
- [15] Lisa Hutschenreiter, Stefan Haller, Lorenz Feineis, Carsten Rother, Dagmar Kainmüller, and Bogdan Savchynskyy. Fusion moves for graph matching. In *Proceedings of the IEEE/CVF International Conference on Computer Vision*, pages 6270–6279, 2021. 2
- [16] B Jiang, P Sun, J Tang, and B Luo. Glnet: Graph learning-matching networks for feature matching. *arXiv preprint arXiv:1911.07681*, 2019. 2, 6, 7
- [17] Max Kahl, Sebastian Stricker, Lisa Hutschenreiter, Florian Bernard, and Bogdan Savchynskyy. Unlocking the potential of operations research for multi-graph matching. *arXiv preprint arXiv:2406.18215*, 2024. 2
- [18] Diederik P Kingma. Adam: A method for stochastic optimization. *arXiv preprint arXiv:1412.6980*, 2014. 5
- [19] Eugene L Lawler. The quadratic assignment problem. *Management science*, 9(4):586–599, 1963. 2

- [20] Yijie Lin, Mouxing Yang, Jun Yu, Peng Hu, Changqing Zhang, and Xi Peng. Graph matching with bi-level noisy correspondence. In *Proceedings of the IEEE/CVF international conference on computer vision*, pages 23362–23371, 2023. 1, 2, 3, 5, 7
- [21] Philipp Lindenberger, Paul-Edouard Sarlin, and Marc Pollefeys. Lightglue: Local feature matching at light speed. In *Proceedings of the IEEE/CVF International Conference on Computer Vision*, pages 17627–17638, 2023. 3
- [22] Ze Liu, Yutong Lin, Yue Cao, Han Hu, Yixuan Wei, Zheng Zhang, Stephen Lin, and Baining Guo. Swin transformer: Hierarchical vision transformer using shifted windows. In *Proceedings of the IEEE/CVF international conference on computer vision*, pages 10012–10022, 2021. 1, 3, 5
- [23] Ilya Loshchilov, Cheng-Ping Hsieh, Simeng Sun, and Boris Ginsburg. ngpt: Normalized transformer with representation learning on the hypersphere. *arXiv preprint arXiv:2410.01131*, 2024. 1, 2, 3, 4
- [24] Iaroslav Melekhov, Aleksei Tiulpin, Torsten Sattler, Marc Pollefeys, Esa Rahtu, and Juho Kannala. Dgc-net: Dense geometric correspondence network. In *2019 IEEE Winter Conference on Applications of Computer Vision (WACV)*, pages 1034–1042. IEEE, 2019. 3
- [25] Pascal Mettes, Elise Van der Pol, and Cees Snoek. Hyper-spherical prototype networks. *Advances in neural information processing systems*, 32, 2019. 1, 2, 5
- [26] Juhong Min, Jongmin Lee, Jean Ponce, and Minsu Cho. Spair-71k: A large-scale benchmark for semantic correspondence. *arXiv preprint arXiv:1908.10543*, 2019. 6, 7
- [27] Aaron van den Oord, Yazhe Li, and Oriol Vinyals. Representation learning with contrastive predictive coding. *arXiv preprint arXiv:1807.03748*, 2018. 1, 2, 3, 4
- [28] Deepti Pachauri, Risi Kondor, and Vikas Singh. Solving the multi-way matching problem by permutation synchronization. *Advances in neural information processing systems*, 26, 2013. 2
- [29] Akshay Gadi Patil, Manyi Li, Matthew Fisher, Manolis Savva, and Hao Zhang. Layoutgm: Neural graph matching for structural layout similarity. In *Proceedings of the IEEE/CVF Conference on Computer Vision and Pattern Recognition*, pages 11048–11057, 2021. 7
- [30] Qibing Ren, Qingquan Bao, Runzhong Wang, and Junchi Yan. Appearance and structure aware robust deep visual graph matching: Attack, defense and beyond. In *Proceedings of the IEEE/CVF Conference on Computer Vision and Pattern Recognition*, pages 15263–15272, 2022. 1, 2, 3, 5, 7
- [31] Michal Rolínek, Paul Swoboda, Dominik Zietlow, Anselm Paulus, Vít Musil, and Georg Martius. Deep graph matching via blackbox differentiation of combinatorial solvers. In *Computer Vision—ECCV 2020: 16th European Conference, Glasgow, UK, August 23–28, 2020, Proceedings, Part XXVIII 16*, pages 407–424. Springer, 2020. 1, 2, 3, 5, 6, 7
- [32] Paul-Edouard Sarlin, Daniel DeTone, Tomasz Malisiewicz, and Andrew Rabinovich. SuperGlue: Learning feature matching with graph neural networks. In *Proceedings of the IEEE/CVF conference on computer vision and pattern recognition*, pages 4938–4947, 2020. 3
- [33] Karen Simonyan and Andrew Zisserman. Very deep convolutional networks for large-scale image recognition. *arXiv preprint arXiv:1409.1556*, 2014. 1, 8
- [34] Jiaming Sun, Zehong Shen, Yuang Wang, Hujun Bao, and Xiaowei Zhou. Loftr: Detector-free local feature matching with transformers. In *Proceedings of the IEEE/CVF conference on computer vision and pattern recognition*, pages 8922–8931, 2021. 3
- [35] Paul Swoboda, Carsten Rother, Hassan Abu Alhaja, Dagmar Kainmuller, and Bogdan Savchynskyy. A study of lagrangean decompositions and dual ascent solvers for graph matching. In *Proceedings of the IEEE conference on computer vision and pattern recognition*, pages 1607–1616, 2017. 2
- [36] Paul Swoboda, Ashkan Mokarian, Christian Theobalt, Florian Bernard, et al. A convex relaxation for multi-graph matching. In *Proceedings of the IEEE/CVF Conference on Computer Vision and Pattern Recognition*, pages 11156–11165, 2019. 2
- [37] Lorenzo Torresani, Vladimir Kolmogorov, and Carsten Rother. A dual decomposition approach to feature correspondence. *IEEE transactions on pattern analysis and machine intelligence*, 35(2):259–271, 2012. 1, 2
- [38] A Vaswani. Attention is all you need. *Advances in Neural Information Processing Systems*, 2017. 4
- [39] Marin Vlastelica, Anselm Paulus, Vít Musil, Georg Martius, and Michal Rolínek. Differentiation of blackbox combinatorial solvers. *arXiv preprint arXiv:1912.02175*, 2019. 2
- [40] Runzhong Wang, Junchi Yan, and Xiaokang Yang. Learning combinatorial embedding networks for deep graph matching. In *Proceedings of the IEEE/CVF international conference on computer vision*, pages 3056–3065, 2019. 2, 6, 7
- [41] Runzhong Wang, Junchi Yan, and Xiaokang Yang. Neural graph matching network: Learning lawler’s quadratic assignment problem with extension to hypergraph and multiple-graph matching. *IEEE Transactions on Pattern Analysis and Machine Intelligence*, 44(9):5261–5279, 2021. 2, 6, 7
- [42] Tianshu Yu, Runzhong Wang, Junchi Yan, and Baoxin Li. Learning deep graph matching with channel-independent embedding and hungarian attention. In *International conference on learning representations*, 2019. 2, 6, 7
- [43] Sangdoon Yun, Dongyoon Han, Seong Joon Oh, Sanghyuk Chun, Junsuk Choe, and Youngjoon Yoo. Cutmix: Regularization strategy to train strong classifiers with localizable features. In *Proceedings of the IEEE/CVF international conference on computer vision*, pages 6023–6032, 2019. 5
- [44] Andrei Zanfir and Cristian Sminchisescu. Deep learning of graph matching. In *Proceedings of the IEEE conference on computer vision and pattern recognition*, pages 2684–2693, 2018. 2
- [45] Hongyi Zhang, Moustapha Cisse, Yann N Dauphin, and David Lopez-Paz. mixup: Beyond empirical risk minimization. *arXiv preprint arXiv:1710.09412*, 2017. 5
- [46] Zhen Zhang and Wee Sun Lee. Deep graphical feature learning for the feature matching problem. In *Proceedings of the IEEE/CVF International Conference on Computer Vision*, pages 5087–5096, 2019. 2

- [47] Zhun Zhong, Liang Zheng, Guoliang Kang, Shaozi Li, and Yi Yang. Random erasing data augmentation. In *Proceedings of the AAAI conference on artificial intelligence*, pages 13001–13008, 2020. [5](#)